NJC

COMMUNICATION

View Article Online
View Journal | View Issue

Cite this: *New J. Chem.*, 2025, **49**, 19086

Received 12th September 2025,
Accepted 16th October 2025

DOI: 10.1039/d5nj03660g

rsc.li/njc

"Anti-electrostatic" (inter-anion) chalcogen bonding interactions†

Margarita Yanbaeva, ‡[a] Tim Steinke, ‡[a] Elric Engelage, [a] Robert Weiss*[b] and Stefan M. Huber *[a]

In this work, the ability of 1,2-bis(dicyanomethylene)-cyclopropanide substituents to enable inter-anion interactions has been expanded to chalcogen bonding. An anionic selenium-based chalcogen-bond donor featuring this ligand displays "anti-electrostatic" interactions in the solid state. Three polymorphic structures of associates with both mono- and biaxial binding modes are discussed.

Noncovalent interactions (NCIs) such as halogen[1] (XB), chalcogen[2] (ChB) and pnictogen[3] (PnB) bonding have received increased interest in the last decades, and based on the anisotropic electrostatic potential of the interacting atom, they have sometimes collectively been termed "σ-hole interactions".[4] These NCIs have established themselves as a flexible tool in various fields like crystal engineering,[5] catalysis,[6] ion recognition[7] and biochemistry.[8] Electrostatics are considered to play a crucial role in the formation of these bonds,[9] however, components contributing to the interaction energies are not limited to simple electrostatic attraction.[10] Several other factors must be taken into account, including dispersion, polarization or charge-transfer§.[11] "Anti-electrostatic" interactions between ions of like charge represent one of the key examples demonstrating the importance of the latter contributions.

In fact, several studies on this counterintuitive phenomenon have been put forth in recent years,[12] and an even broader selection of examples emerges as previously reported data is re-evaluated with this concept in mind¶.[13] Nevertheless, experimental findings are limited in scope, especially those involving the interactions between organic molecules.

One of the first examples of "anti-electrostatic" halogen bonding (AEXB) between structurally distinct species was previously reported by our group.[14] The anionic iodinated cyclopropanide XB donor **1** and cyclopropanide-substituted imidazole species **2** (see Fig. 1, top) have displayed halide adduct formation and self-association, respectively.

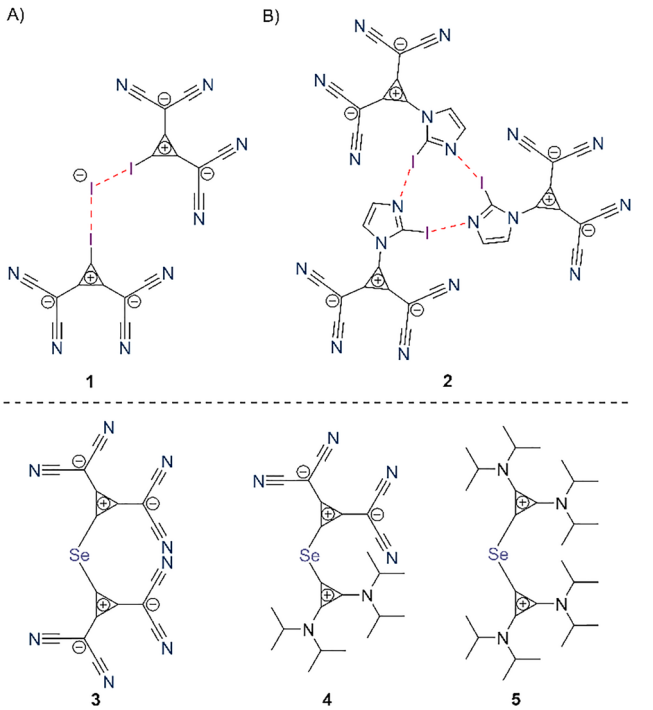

Fig. 1 Top: Previously reported cases of "anti-electrostatic" halogen bonded aggregates of 1,2-bis(dicyanomethylene)-cyclopropanide-containing synthons in the solid state: (A) – 2 : 1 anion binding and (B) – trimer formation. For (A): $d_{I\cdots I}$ = 85% Σr_{ω}, in (B): $d_{I\cdots N}$ = 79–81% Σr_{ω}. Cations omitted for clarity. Bottom: Known cyclopropanide- and cyclopropenium-substituted chalcogen compounds. Counterions omitted for clarity.

Since halogen and chalcogen bonding share many similarities, the concept of "anti-electrostatic" bonding could potentially also be expanded to ChB ("AEChB").[15] Obvious candidate structures to realize these contacts are organochalcogen compounds bearing

[a] *Fakultät für Chemie und Biochemie, Ruhr-Universität Bochum Universitätsstraße 150, 44801 Bochum, Germany. E-mail: stefan.m.huber@rub.de*
[b] *Institut für Organische Chemie, Friedrich-Alexander-Universität Erlangen-Nürnberg Henkestraße 42, 91054 Erlangen, Germany. E-mail: robert.weiss@chemie-uni-erlangen.de*

† Dedicated to Professor Resnati, celebrating a career in fluorine and noncovalent chemistry on the occasion of his 70th birthday.

‡ These authors contributed equally to this work.

cyclopropanide moieties analogously to the reported halogen-bond donors.

Both cationic cyclopropenium- and anionic cyclopropanide-substituted selenium compounds (**3**–**5**) have previously been reported by Seitz and co-workers.[16] The crystal structure of the mixed species **4** is literature-known; however, no further analysis of the intermolecular interactions in the solid state has been performed to date.

Following up on our previous investigations regarding "anti-electrostatic" noncovalent interactions, we herein present, to the best of our knowledge, the first example of inter-anion chalcogen bonding in the solid state.

Results and discussion

Anionic 1,2-bis(dicyanomethylene)cyclopropanide derivative **7** was prepared from commercially available trichloroethylene over four steps following previously established procedures.[14] The chalcogen-bond donor **8** was subsequently synthesized from phenylselenyl chloride with 85% yield. This reaction further underlines the autoumpolung[17] properties of **7**, as the transformation likely occurs *via* a nucleophilic attack of the ambiphilic carbon of the cyclopropanide moiety on the selenium (see Scheme 1).

During crystallization experiments with compound **8** without further additives, two different polymorphic structures of supramolecular aggregates could be identified. Crystals suitable for analysis were obtained *via* vapor diffusion from THF with cyclohexane as antisolvent, or *via* slow evaporation from DCM, with the individual structures discussed below.

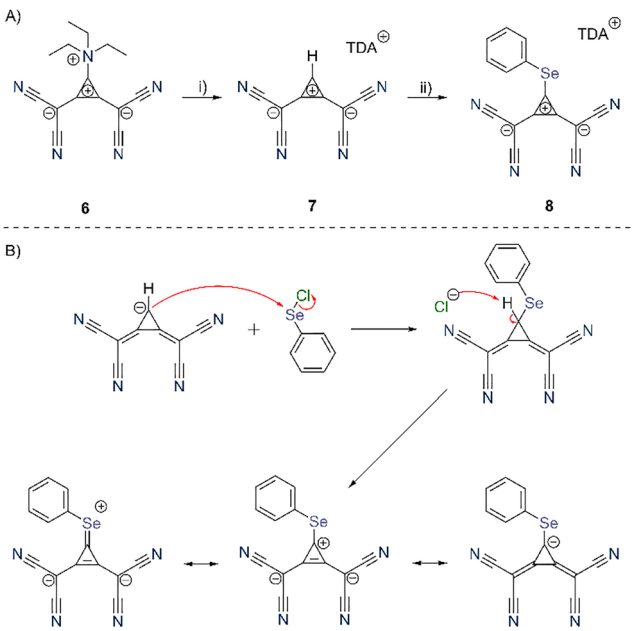

Scheme 1 (A) Synthesis of the anionic chalcogen bond donor **8**; TDA – tris(dimethylamino)cyclopropenylium; (i) (1) $NaBH_4$, MeOH, 0 °C → r.t., 2 h (2) H_2O/DCM, TDACl; (ii) (1) PhSeCl. THF, rt, 14 h, (2) H_2O/DCM, TDACl; (B) proposed mechanism of the formation of **8** (involving polarity inversion) and possible resonance structures of **8**. Cations omitted for clarity.

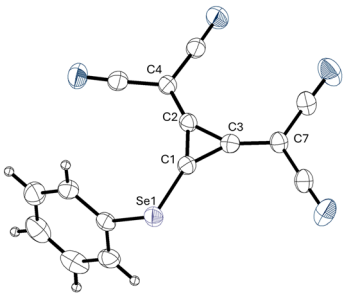

Bond	Crystal	B3LYP	M062X
Se1-C1	1.862	1.866	1.858
C1-C2	1.374	1.373	1.374
C1-C3	1.373	1.378	1.369
C2-C3	1.411	1.413	1.410
C2-C4	1.381	1.381	1.383
C3-C7	1.378	1.386	1.377

Fig. 2 Selected average bond lengths of **8**. Ellipsoids set at 50% probability. TDA cations omitted for clarity. Geometry optimization performed with B3LYP[20] and M06-2×[21] functionals, applying def2TZVP(D)[22] basis set.

A summary of mean bond lengths of all unique instances of **8** as well as values obtained from gas phase geometry optimizations on different levels of theory are presented in Fig. 2. Overall, high agreement between experimental and theoretical data can be observed. The C–C distances are representative of a highly conjugated structure, as the values are close to those present in benzene (1.390 Å).[18] Notably, the C2–C3 bond is slightly longer at 1.411 Å, while the Se1–C1 distance is, in turn, shorter than a typical carbon–selenium single bond.[19] The former observation is more in line with the right resonance structure of Scheme 1B, while the latter seems to indicate a contribution from the left one. The short Se-C distance could also be indicative of an n → σ* interaction of the anionic carbon into the Se–C_{Ph} σ* orbital, though.

The electronic nature of the chalcogen-bond donor was further investigated with the help of an electrostatic potential (ESP) map, which was calculated at B3LYP/def2TZVP(D) level of theory. Overall, a rather homogeneous distribution of the negative charge is observed, with no areas with positive potential present (see Fig. 3). Nevertheless, a region with relatively lower electron density (blue) is seen opposite to the cyclopropanide substituent, while no such area is visible along the phenyl substituent's axis. The cyano groups feature the most negative electrostatic potential (displayed in red) and are thus capable of acting as chalcogen-bond acceptors.

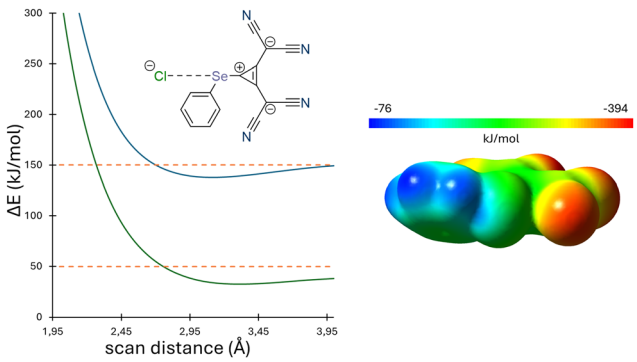

Fig. 3 Left: Total energy profile of the scan of the Cl···Se distance in the **8**-Cl adduct in the gas phase (blue) and in MeCN solution (green) calculated at M06-2X level of theory. Right: Electrostatic potential of **8** mapped on the 0.001 electron/Bohr^3 isosurface of electronic density.

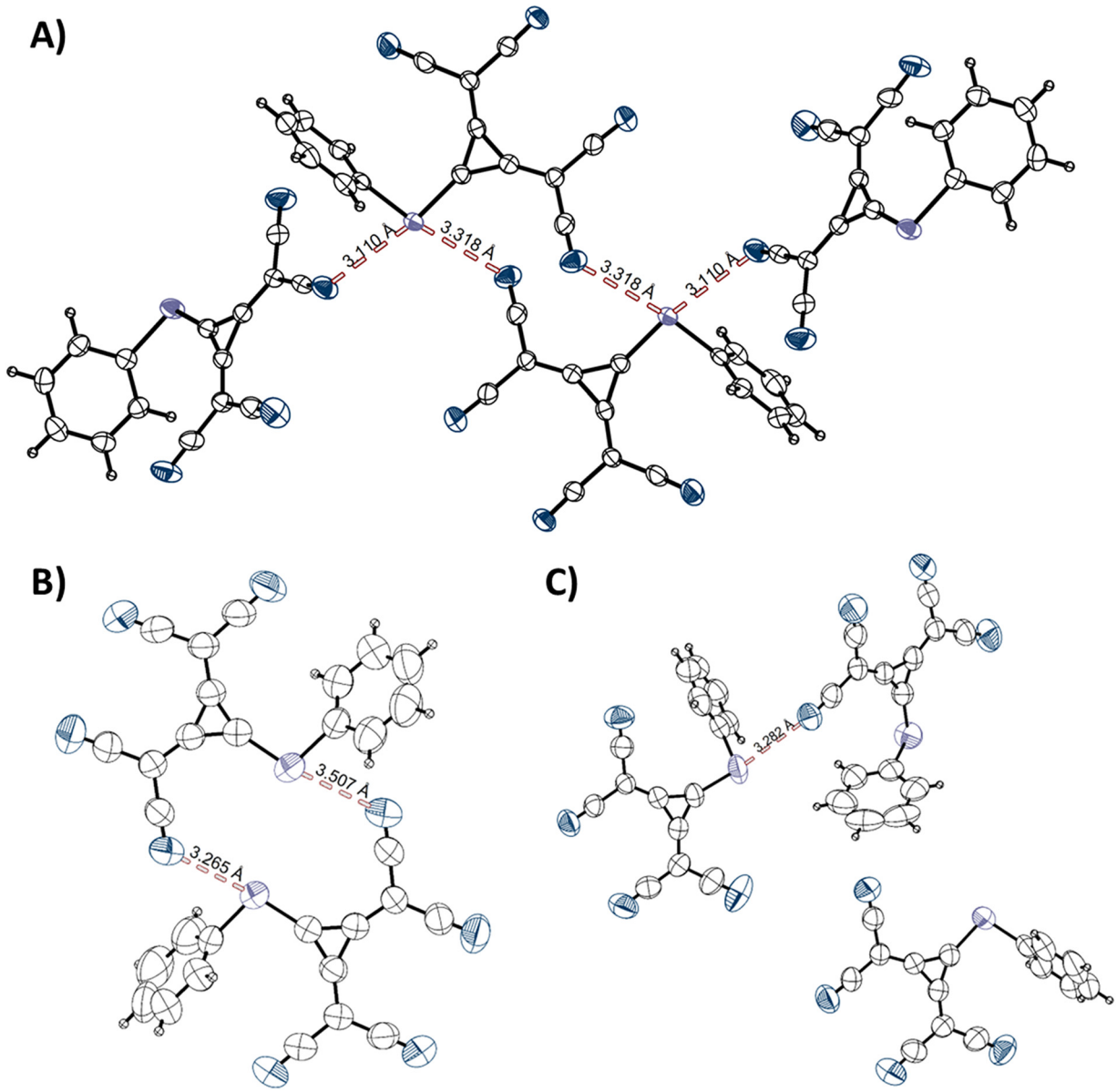

Fig. 4 Single crystal X-ray structure of **8**: (A) biaxial binding; (B) and (C) monoaxial binding. The sum of van der Waals radii for selenium and nitrogen amounts to 3.45 Å. TDA cations omitted for clarity. Ellipsoids set at 50% probability. In both cases of monoaxial binding, the formation of the chalcogen-bond is observed in the elongation of the cyclopropanide–selenium bond. In (A), suitable interactions are detected along both axes. The bond formed in the elongation of the cyclopropanide substituent is significantly shorter. A summary of observed bond lengths and angles can be found in Table 1.

Additionally, total energy profiles of the Cl···Se distance scans were plotted at the M06-2X/def2TZVP(D) level of theory to evaluate the thermodynamics of a potential non-isostructural interaction between the anion of **8** and chloride (Fig. 3). The formation of the adduct in both gas phase and acetonitrile is endothermic; a result expected from an anion–anion interaction. Still, well depths (the differences between the energies of the complex at minima and extended distances) of −11.6 kJ mol^{-1} and −5.1 kJ mol^{-1} are observed in the gas phase and in acetonitrile solution, respectively. These minima are located at 3.1 Å (85% vdW) and 3.2 Å (88% vdW), distances that are typical for a chalcogen-bonded adduct.

In an attempt to obtain chalcogen bonding complexes with halides, co-crystallization experiments with one equivalent of tris(dimethylamino)-cyclopropenylium chloride (TDACl) were repeated under the same conditions used previously.

Table 1 Selected geometric parameters of the chalcogen bonds in the crystal structures presented in Fig. 4. Most favourable values marked in bold

Bond	dSe···N, [Å]	Σr_{ω}, [%]	∢C–Se···N, [°]
A_a (Se2···N2)	**3.110**	**90**	168.7
A_b (Se2···N8)	3.318	96	170.4
B (Se1···N6)	3.265	95	154.6
C (Se2···N11)	3.282	95	**172.4**

These, however, only yielded an additional polymorph of **8**, as well as isolated TDACl single crystals.

Crystal structures of the three polymorphs of **8** are depicted in Fig. 4. A major difference between ChB and neutral XB donors is the ability of the former to form non-covalent bonds along both substituents axes, so-called biaxial binding. Still, adduct formation is often only observed along one of these, usually opposite the more electronegative substituent.[23] Here, both modes are observed.

From the conceptual standpoint, polymorph **A**, which was obtained from slow evaporation from DCM, provides the most information due to its biaxial binding motif. This tetraanionic aggregates presented in Fig. 4A display the longest chain formed within the crystal structure. As seen from the atom labelling, the anions in the smallest asymmetrical unit represent half of that chain, and all the anionic moieties are a part of those superstructures (see Fig. S7 and S8 in SI).

Due to packing effects, no chalcogen bond is formed in the elongation of both axes of the terminal Se atoms. Those molecules are bound to anions of neighbouring chains by weak N–H contacts (Fig. S10 in SI). The corresponding cations are located above and below the cyclopropanide moieties, displaying π–π interactions and short contacts. For the inner moieties, a direct comparison between the chalcogen bond lengths along the different substituents axes can be drawn. A shortening of about 6% of the sum of vdW radii is observed for the cyclopropanide axis compared to the phenyl one despite the net negative charge of the former. Additionally, this structure contains the shortest chalcogen bond amongst the herein reported, corresponding to 90% vdW radii (see Table 1 for a summary of relevant parameters).

The monoaxial binding in structures **B** and **C** only occurs along the elongation of the selenium-cyclopropanide bond, which is in line with the differences of ChBs in **A** discussed above. It indicates that the cyclopropanide substituent, despite its anionic nature, creates the superior ChB axis.

The dimeric structure of **B** was obtained from vapor diffusion experiments with THF/cyclohexane. All the selenium-containing moieties partake in the dimer formation, and no other interactions apart from these short contacts and alternating π stacking between the cations and the cyclopropanide part of the anions can be observed. The latter form offset columns (see SI, Fig. S11 and S12). The chalcogen bond here amounts to 95% vdW, comparably longer than the one observed in structure **A** for the cyclopropanide substituent. Additionally, although the orientation of the molecules would suggest a rather symmetric motif in structure **B** with both selenium atoms forming a bond with the corresponding nitrogens, a slight distortion is present. The distance of the second Se–N pair amounts to 3.507 Å, 101% vdW, at or beyond the border of a chalcogen bond. A slight offset between the neighboring planes results in a relatively low directionality of the chalcogen bonds.

The final polymorph **C** was obtained from gas diffusion experiments with THF/cyclohexane with 1 eq. of TDACl additive. Remarkably, only one of the individual anion pairs in the smallest asymmetrical unit is displaying chalcogen bonding (see Fig. S13). Here, a Se–N bond distance of 95% vdW is observed. This is the most directional interaction amongst the observed structures, with a C–Se–N angle of 172.4°. A third moiety, which does not display any intermolecular interactions besides short contacts towards the hydrogens of the adjacent phenyl groups of other anions and π stacking with the TDA cations, is present. Similarly to the other structures, an alternating pattern in the π-stacking between the positively and negatively charged fragments is observed.

While no experimental data on ''anti-electrostatic'' chalcogen bonding is reported to the best of our knowledge, numerous studies involving neutral and cationic donors in the solid state have been presented over the years, with individual results,[24] as well as overarching data bank surveys[25] being available. The values observed in the anionic systems presented above are comparable with those literature-known parameters – despite their unfavourable electrostatic contribution.

Conclusions

In conclusion, we present a novel chalcogen-bond donor based on the 1,2-bis(dicyanomethylene)cyclopropanide moiety, which is capable of inter-anion bonding. Three polymorphs featuring varying self-aggregation patterns could be described. The interaction parameters are comparable to previously reported complexes of dicationic selenium-based donors with neutral and cationic Lewis bases. Since selenium is known to form weaker chalcogen bonds compared to its heavier homologue, we anticipate that the preparation of cyclopropanide-substituted tellurium donors would allow to fully realize the potential of AEChB. These studies are currently ongoing.

Conflicts of interest

There are no conflicts to declare.

Data availability

The data supporting this article have been included as part of the Supplementary information (SI). Supplementary information: Additional data on experimental procedures, crystal structures, spectra and computational details is presented in the SI. See DOI: **https://doi.org/10.1039/d5nj03660g**.

CCDC 2477887–2477889 contain the supplementary crystallographic data for this paper.[27a–c]

Notes and references

§ While we prefer to call the contribution arising from the overlap of orbitals ''charge-transfer'', it has also been postulated that its effect can solely be explained by polarization.[26] This discussion is outside the scope of this study.

¶ For an early example of an inter-*cation* AECB, see: R. Laitinen, R. Steudel, R. Weiss, *J. Chem. Soc., Dalton Trans.* **1986**, 1095.

1 P. R. Varadwaj, A. Varadwaj, H. M. Marques and K. Yamashita, *Cryst. Growth Des.*, 2024, **24**, 5494–5525.

2 C. B. Aakeroy, D. L. Bryce, G. R. Desiraju, A. Frontera, A. C. Legon, F. Nicotra, K. Rissanen, S. Scheiner, G. Terraneo, P. Metrangolo and G. Resnati, *Pure Appl. Chem.*, 2019, **91**, 1889–1892.
3 G. Resnati, D. L. Bryce, G. R. Desiraju, A. Frontera, I. Krossing, A. C. Legon, P. Metrangolo, F. Nicotra, K. Rissanen, S. Scheiner and G. Terraneo, *Pure Appl. Chem.*, 2024, **96**, 135–145.
4 T. Clark, M. Hennemann, J. S. Murray and P. Politzer, *J. Mol. Model.*, 2007, **13**, 291–296.
5 (*a*) P. Metrangolo and G. Resnati, *Cryst. Growth Des.*, 2012, **12**, 5835–5838; (*b*) R. Siddiqui, J. Rani, H. M. Titi and R. Patra, *Coord. Chem. Rev.*, 2024, **517**, 215994.
6 D. Jovanovic, M. Poliyodath Mohanan and S. M. Huber, *Angew. Chem., Int. Ed.*, 2024, **63**, e202404823.
7 G. Berger, P. Frangville and F. Meyer, *Chem. Commun.*, 2020, **56**, 4970–4981.
8 M. G. Walker, C. G. Mendez and P. S. Ho, *Chem. – Asian J.*, 2023, **18**, e202300026.
9 P. Politzer, J. S. Murray and T. Clark, *Phys. Chem. Chem. Phys.*, 2010, **12**, 7748–7757.
10 (*a*) P. Politzer, P. Lane, M. C. Concha, Y. Ma and J. S. Murray, *J. Mol. Model.*, 2007, **13**, 305–311; (*b*) P. Politzer, J. S. Murray and M. C. Concha, *J. Mol. Model.*, 2007, **13**, 643–650; (*c*) L. de Azevedo Santos, T. C. Ramalho, T. A. Hamlin and F. M. Bickelhaupt, *Chem. – Eur. J.*, 2023, **29**, e202203791; (*d*) A. Lara, A. Sterling, A. Aldossary and M. Head-Gordon, *ChemRxiv*, 2024, DOI: **10.26434/chemrxiv-2024-t26hd**.
11 (*a*) H. A. Bent, *Chem. Rev.*, 1968, **68**, 587–648; (*b*) A. E. Reed, F. Weinhold, R. Weiss and J. Macheleid, *J. Phys. Chem.*, 1985, **89**, 2688–2694.
12 (*a*) C. Wang, Y. Fu, L. Zhang, D. Danovich, S. Shaik and Y. Mo, *J. Comput. Chem.*, 2018, **39**, 481–487; (*b*) Z. Zhu, G. Wang, Z. Xu, Z. Chen, J. Wang, J. Shi and W. Zhu, *Phys. Chem. Chem. Phys.*, 2019, **21**, 15106–15119.
13 J. M. Holthoff, R. Weiss, S. V. Rosokha and S. M. Huber, *Chem. – Eur. J.*, 2021, **27**, 16530–16542.
14 J. M. Holthoff, E. Engelage, R. Weiss and S. M. Huber, *Angew. Chem., Int. Ed.*, 2020, **59**, 11150–11157.
15 D. Fan, L. Chen, C. Wang, S. Yin and Y. Mo, *J. Chem. Phys.*, 2021, **155**, 234302.
16 R. Allmann, F.-J. Kaiser, M. Krestel and G. Seitz, *Angew. Chem., Int. Ed. Engl.*, 1986, **25**, 183–184.
17 R. Weiss, S. Reichel, M. Handke and F. Hampel, *Angew. Chem., Int. Ed.*, 1998, **37**, 344–347.
18 I. Heo, J. C. Lee, B. R. Özer and T. Schultz, *J. Phys. Chem. Lett.*, 2022, **13**, 8278–8283.
19 P. Wonner, L. Vogel, M. Düser, L. Gomes, F. Kniep, B. Mallick, D. B. Werz and S. M. Huber, *Angew. Chem., Int. Ed.*, 2017, **56**, 12009–12012.
20 A. D. Becke, *J. Chem. Phys.*, 1993, **98**, 5648–5652.
21 Y. Zhao and D. G. Truhlar, *Theor. Chem. Acc.*, 2008, **120**, 215–241.
22 P. J. Stephens, F. J. Devlin, C. F. Chabalowski and M. J. Frisch, *J. Phys. Chem.*, 1994, **98**, 11623–11627.
23 S. Scheiner, *Chem. Phys. Chem.*, 2023, **24**, e202200936.
24 (*a*) T. Steinke, E. Engelage and S. M. Huber, *Acta Crystallogr., Sect. C: Cryst. Struct. Commun.*, 2023, **79**, 26–35; (*b*) P. Wonner, L. Vogel, M. Düser, L. Gomes, F. Kniep, B. Mallick, D. B. Werz and S. M. Huber, *Angew. Chem., Int. Ed.*, 2017, **56**, 12009–12012.
25 (*a*) A. Frontera and A. Bauzá, *Crystals*, 2021, 11; (*b*) E. R. Tiekink, *Coord. Chem. Rev.*, 2021, **427**, 213586.
26 T. Clark and A. Heßelmann, *Phys. Chem. Chem. Phys.*, 2018, **20**, 22849–22855.
27 (*a*) CCDC 2477887: Experimental Crystal Structure Determination, 2025, DOI: **10.5517/ccdc.csd.cc2ph4kx**; (*b*) CCDC 2477888: Experimental Crystal Structure Determination, 2025, DOI: **10.5517/ccdc.csd.cc2p5fw6**; (*c*) CCDC 2477889: Experimental Crystal Structure Determination, 2025, DOI: **10.5517/ccdc.csd.cc2p5fx7**.

